Eurasian Journal of Physics and Functional Materials

Volume 3 | Number 4

Article 3

Pages: 307 - 318

12-22-2019

Shell model calculations for deformed Li isotopes

A. K. Azhibekov
Gumilyov Eurasian National University ,Kazakhstan

V. V. Samarin
Joint Institute for Nuclear Research ,Russian Federation

K. A. Kuterbekov
Gumilyov Eurasian National University ,Kazakhstan

M. A. Naumenko
Joint Institute for Nuclear Research ,Russian Federation ,

Eurasian Journal of Physics and Functional Materials

2019, 3(4), 307-318

Shell model calculations for deformed Li isotopes

A.K. Azhibekov*[,1,2], V.V. Samarin[2,3],
K.A. Kuterbekov[1], M.A. Naumenko[2]

[1]L.N. Gumilyov Eurasian National University, Nur-Sultan, Kazakhstan

[2]Joint Institute for Nuclear Research, Dubna, Russia

[3]Dubna State University, Dubna, Russia

E-mail: azhibekoaidos@mail.ru

DOI: **10.29317/ejpfm.2019030403**
Received: 25.11.2019 - after revision

The nuclear shell model and its application to studying the structure of nuclei with deformed and spherical shapes are discussed. Calculations of level energies and wave functions in the shell model of deformed and spherical nuclei are performed for ^{7,8,11}Li nuclei. A detailed calculation scheme for solving the radial Schrödinger equation is presented.

Keywords: shell model calculations, deformed and spherical nuclei, Li isotopes.

Introduction

Low-energy reactions with the participation of tritium, helium, lithium, and beryllium nuclei [1] constitute a large part of the nuclear reactions that have been and continue to be studied. Reactions with Li isotopes are of considerable interest from several points of view [2]. With a ratio of the number of neutrons to the number of protons that varies from 1 to 2.67, $^{6-11}$Li nuclei have a significantly different structure and provide a unique opportunity for testing different microscopic models [3]. Knowledge of the properties and the wave function of the ground states of lithium nuclides is necessary for a theoretical description of reactions with their participation. Outer nucleons in the simplest spherical shell models of ^{6}Li$(n+p+\alpha)$ and ^{7}Li $(n+n+p+\alpha)$ configurations [1-7] in the field of

the nuclear core (α cluster) occupy the $1p_{3/2}$ state and exhibit the properties of clusters (deuteron and triton, respectively) [8]. Li isotopes are deformed [9], therefore to study the structure these nuclei it is necessary to take into account the parameters of quadrupole β_2 and hexadecapole β_4 deformations [10]. For studying Li isotopes, we used the shell model of deformed nuclei. At the same time, we demonstrate that the shell model of spherical nuclei may also be used for approximate description of the weakly bound external neutrons in ^{11}Li [11] and ^{8}Li nuclei.

The shell model of the nucleus assumes a self-consistent field of nuclear forces, i.e., real forces acting between nucleons [10, 12]. There is a repulsive region in the nucleus (strong short-range correlations) that prevents nucleons from getting close to each other. Therefore, the formalism of the Hartree-Fock method, in which all dynamic correlations are neglected, cannot be applied to a system containing short-range correlation [13]. In the initial approximation, self-consistent field can be replaced by a common force center for all nucleons. Thus, it reduces the problem of many bodies to the problem of one particle moving in this field. By solving the Schrödinger equation for the motion of a nucleon in a mean field, we obtain a system of possible bound states with each state corresponding to a certain level of energy. For the first time, the idea concerning the nuclear shell structure with spin-orbit interaction was proposed M. Göppert-Mayer and J. Hans D. Jensen [14]. The nucleons, as particles with spin 1/2, obey the Pauli exclusion principle, according to which in each state can be no more than one particle. Therefore, nucleons in the nucleus consistently fill the energy levels, starting from the lowest. It is well known that the shell model with spin-orbit interaction explained the existence of magic numbers in nuclear physics — the fact that elements with atomic weights 2, 8, 20, 28, 50, 82, and 126 were extremely stable.

The shell model of deformed nucleus

For a deformed nucleus with an axially symmetric surface described in a spherical coordinate system by the equation $R = R^{(\mathrm{WS})}(\theta)$, the potential energy of a nucleon is usually represented in the Woods-Saxon form

$$U^{(\mathrm{WS})}(r, \cos\theta) = V_0^{(\mathrm{WS})} \left\{ 1 + \exp\left(\frac{r - R^{(\mathrm{WS})}(\theta)}{a^{(\mathrm{WS})}} \right) \right\}^{-1}, \tag{1}$$

where the shape of a deformed nucleus with dimensionless deformation parameters β_λ for multiplicities $\lambda = 2, 4$ is represented using the decomposition into spherical functions [15]:

$$R^{(\mathrm{WS})}(\theta) = \tilde{R}^{(\mathrm{WS})} \left[1 + \beta_2 Y_{20}(\theta, 0) + \beta_4 Y_{40}(\theta, 0) \right], \tag{2}$$

$$\tilde{R}^{(\mathrm{WS})} = R_0^{(\mathrm{WS})} \left[1 + \frac{3}{4\pi} \left(\beta_2^2 + \beta_4^2 \right) \right]^{-1/3} \tag{3}$$

where $R_0^{(\mathrm{WS})} = r_0^{(\mathrm{WS})} A^{1/3}$, and A is the mass number.

The nucleon states in the field of the axially deformed nucleus may be determined by solving the Schrödinger equation in cylindrical coordinates [16] ρ, φ, z

$$\left[-\frac{\hbar^2}{2m}\Delta + U^{(\mathrm{WS})}(\rho,z) + i\frac{b}{2}\frac{1}{\rho}U_\rho^{(\mathrm{SO})}\frac{\partial}{\partial\varphi}\right]\psi_{1\nu} + \\ + i\frac{b}{2}e^{-i\varphi}\left[i\left(U_\rho^{(\mathrm{SO})}\frac{\partial}{\partial z} - U_z^{(\mathrm{SO})}\frac{\partial}{\partial\rho}\right) - \frac{1}{\rho}U_z^{(\mathrm{SO})}\frac{\partial}{\partial\varphi}\right]\psi_{2\nu} = \varepsilon_\nu\psi_{1\nu}, \tag{4}$$

$$\left[-\frac{\hbar^2}{2m}\Delta + U^{(\mathrm{WS})}(\rho,z) - i\frac{b}{2}\frac{1}{\rho}U_\rho^{(\mathrm{SO})}\frac{\partial}{\partial\varphi}\right]\psi_{2\nu} - \\ i\frac{b}{2}e^{i\varphi}\left[i\left(U_\rho^{(\mathrm{SO})}\frac{\partial}{\partial z} - U_z^{(\mathrm{SO})}\frac{\partial}{\partial\rho}\right) + \frac{1}{\rho}U_z^{(\mathrm{SO})}\frac{\partial}{\partial\varphi}\right]\psi_{1\nu} = \varepsilon_\nu\psi_{2\nu}, \tag{5}$$

where the function $U^{(\mathrm{SO})}(r,\cos\theta)$ corresponds to spin-orbit interaction and has the Woods-Saxon form

$$U^{(\mathrm{SO})}(r,\cos\theta) = V_0^{(\mathrm{SO})}\left\{1+\exp\left(\frac{r-R^{(\mathrm{SO})}(\theta)}{a^{(\mathrm{SO})}}\right)\right\}^{-1}. \tag{6}$$

here m is nucleon mass $U_\rho^{(\mathrm{SO})} \equiv \partial U^{(\mathrm{SO})}\big/\partial\rho$, $U_z^{(\mathrm{SO})} \equiv \partial U^{(\mathrm{SO})}\big/\partial z$, $b = \frac{\kappa}{2}\frac{\hbar^2}{c^2m^2}$, c is speed of light, and κ is the strength constant of the spin-orbit coupling.

It is necessary to supplement equations (4), (5) with the homogeneous boundary conditions at the cylinder surface ($\rho = \rho_0$, $z = z_0 < 0$, and $z = z_M > 0$) chosen in such a way that the distance from it to the surfaces of the nuclei significantly exceeds the range nuclear forces (about 1 fm). The resulting boundary-value problem has a discrete spectrum of energy eigenvalues $\varepsilon_\nu < 0$; values $\varepsilon_\nu > 0$ correspond to the continuous spectrum in an unbounded space. Taking into account axial symmetry of the potential, the normalized particular solutions

$$\iiint\left(\psi^*_{1\mu m_{j_1}}\psi_{1\nu m_{j_2}} + \psi^*_{2\mu m_{j_2}}\psi_{2\nu m_{j_2}}\right)dV = \delta_{\mu\nu}\delta_{m_{j_1}m_{j_2}} \tag{7}$$

can be presented in the form

$$\psi_{1\nu m_j}(\rho,z,\varphi) = (2\pi)^{-1/2} f_{1\nu m_j}(\rho,z)\exp\left(i(m_j-1/2)\varphi\right), \tag{8}$$

$$\psi_{2\nu m_j}(\rho,z,\varphi) = (2\pi)^{-1/2} f_{2\nu m_j}(\rho,z)\exp\left(i(m_j+1/2)\varphi\right), \tag{9}$$

where $m_j = -j, -j+1, \ldots, j$ is the quantum number of the angular-momentum projection onto the nuclear symmetry axis Oz. The probability density P in cylindrical coordinates for neutron levels with quantum numbers ν, m_j is defined as

$$P = \left|\psi_{1\nu m_j}\right|^2 + \left|\psi_{2\nu m_j}\right|^2. \tag{10}$$

For solving the Schrödinger equations (4), (5), we used the method based on expansion of functions f_1 and f_2 into a series of Bessel functions proposed in [16].

In addition, we carried out calculations for the deformed ^{7,8,11}Li nuclei using the NRV Web Knowledge Base [4].

The calculations within the shell model of a deformed nucleus using the method of [16] yielded energies of the upper occupied levels of ^{7,8,11}Li nuclei, which were approximately equal to the experimental neutron separation energies taken with opposite signs [17]. The values of the quadrupole deformation parameter β_2 for ^{7}Li (from –1.024 to –0.934) and for ^{11}Li (–0.636) were obtained from the experimental values of quadrupole moments [9]. In the calculations below, the parameter $\beta_4 = 0$. The resulting neutron level schemes $\varepsilon_\nu\left(|m_j|\right)$ are shown in Figure 1. The Pauli exclusion principle states that no more than two neutrons with $m_j = \pm|m_j|$ can occupy the each level. Two neutrons and two protons at deep lower levels with $|m_j| = 1/2$ corresponding to the level $1s_{1/2}$ of the spherical nucleus belong to a nuclear core similar to a polarized α cluster (see Figure 2a). The two outer neutrons of the ^{7}Li nucleus at the sublevel with the projection of the total momentum on the axis of symmetry of the nucleus $|m_j| = 3/2$, corresponding to level $1p_{1/2}$ of the spherical nucleus (see Figure 2b) are strongly bound with the nuclear core, since the neutron separation energy is 7.25 MeV.

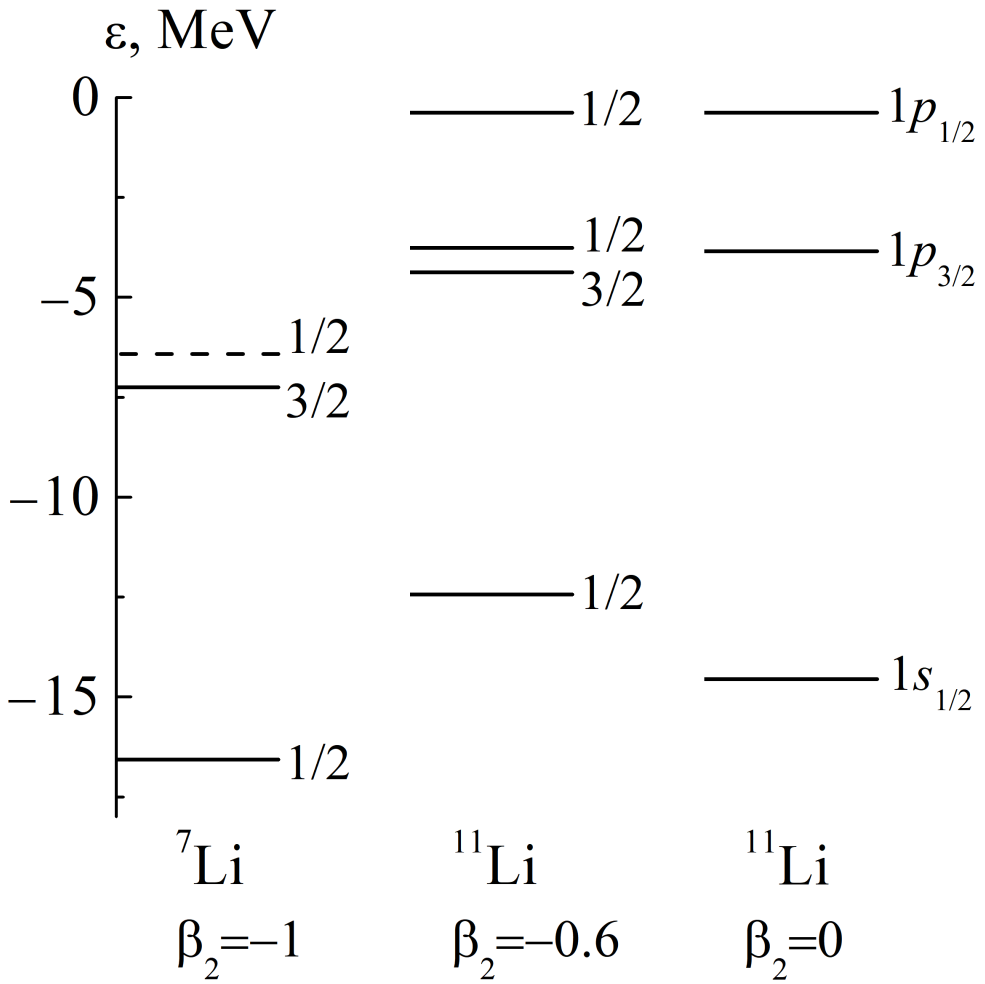

Figure 1. Neutron level schemes for ^{7}Li and ^{11}Li nuclei in the shell model of deformed nucleus and in the shell model of spherical nucleus ^{11}Li. Quantum numbers $|m_j|$ of the angular-momentum projection onto the nuclear symmetry axis Oz are indicated for $\beta_2 \neq 0$. Solid segments are occupied levels; dashed segments are unoccupied levels. Results were obtained using expansion into series of Bessel functions.

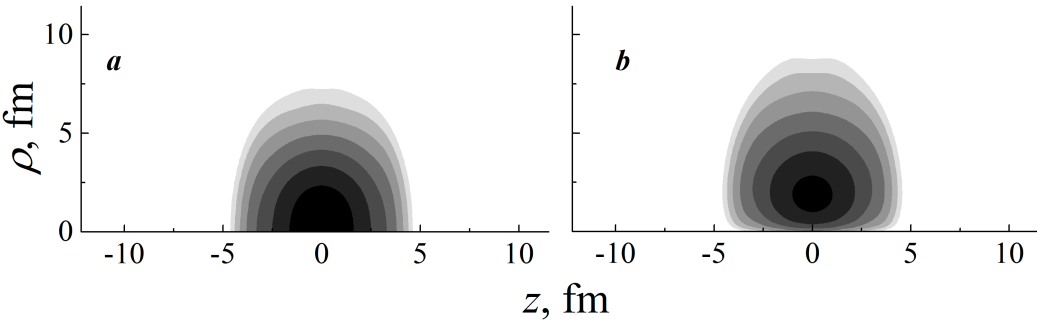

Figure 2. Probability density (here and below in cylindrical coordinates with axis of symmetry Oz) for neutron levels with quantum numbers of the angular-momentum projection onto the nuclear symmetry axis Oz: $|m_j| = 1/2$ (a), $|m_j| = 3/2$ (b) in the shell model of deformed ($\beta_2 = 0.8, \beta_4 = 0$) ^{7}Li nucleus obtained using the NRV Web Knowledge Base [4].

The energies of the sublevels in the deformed ^{11}Li nucleus with $|m_j| = 3/2$ and $|m_j| = 1/2$ corresponding to the level $1p_{1/2}$ of the spherical nucleus are close (see Figure 1). This allows us to use with fair accuracy the spherical shell model for the ^{11}Li nucleus with three occupied neutron shells: $1s_{1/2}$ (in a polarized alpha-cluster core), $1p_{3/2}$ (in the first inner shell), and $1p_{1/2}$ (in the outer halo shell). The probability density for the outer neutron level in the shell model of deformed ^{11}Li nucleus and in the shell model of spherical ^{11}Li nucleus is shown in Figure 3. Outer neutron clouds in the shell model of deformed and spherical nuclei have similar spatial extent. It confirms the possibility of application of the spherical shell model to description of the weakly bound external neutrons in the ^{11}Li nucleus [11].

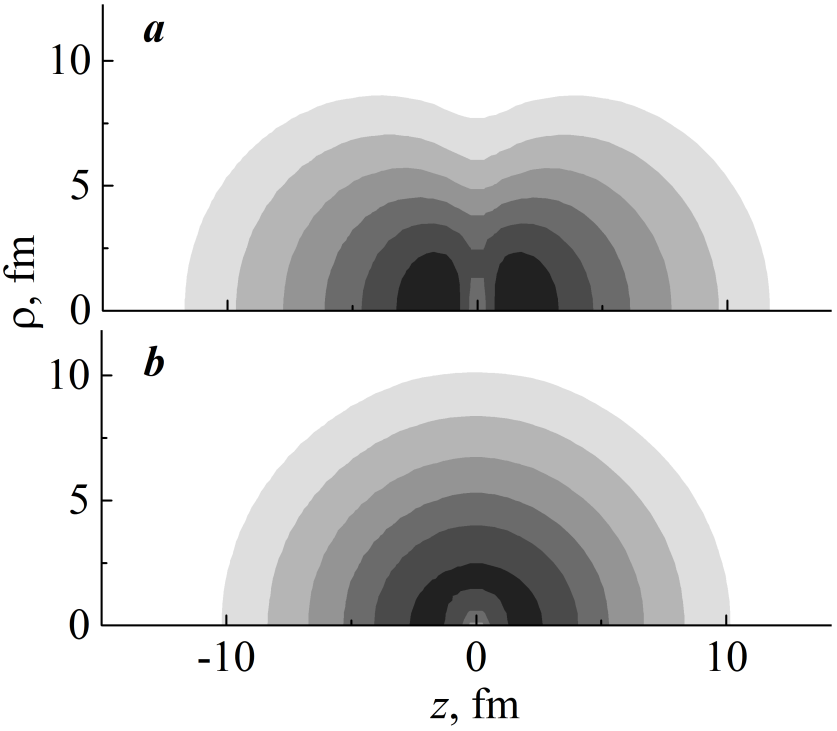

Figure 3. Probability density for for the outer neutron level of ^{11}Li with quantum numbers $|m_j| = 1/2$: (a) $|m_j| = 1/2$ in the shell model of deformed nucleus ($\beta_2 = -0.6, \beta_4 = 0$), (b) in the shell model of spherical nucleus. Results were obtained using expansion into series of Bessel functions.

The absolute values of the quadrupole deformation parameter β_2 for ^{8}Li (from 0.476 to 0.526) and for ^{9}Li (from 0.567 to 0.806) were obtained from the experimental values of quadrupole moments, but the sign of β_2 is unknown [9]. The theoretical dependence of level energies on the deformation parameter β_2 for the ^{8}Li nucleus is shown in Figures 4, 5.

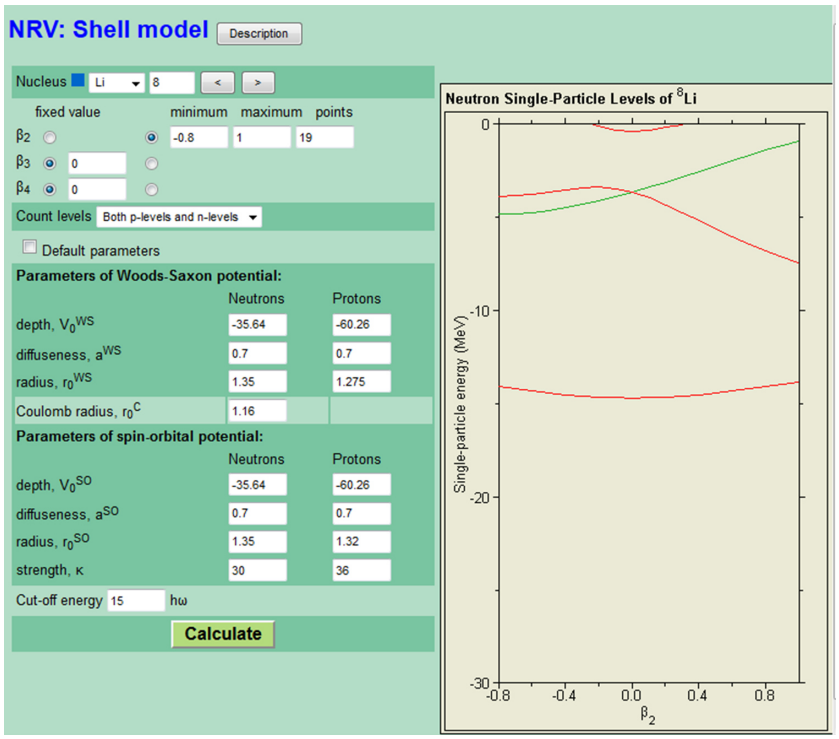

Figure 4. The dependence of level energies on the deformation parameter β_2 for the ^{8}Li nucleus ($\beta_4 = 0$). Calculations were performed using the NRV Web Knowledge Base [4]. Potential parameters are $V_0^{(WS)} = V_0^{(SO)} = -35.64$ MeV, $a^{(WS)} = a^{(SO)} = 0.7$ fm, $r_0^{(WS)} = r_0^{(SO)} = 1.35$ fm, $\kappa = 30$.

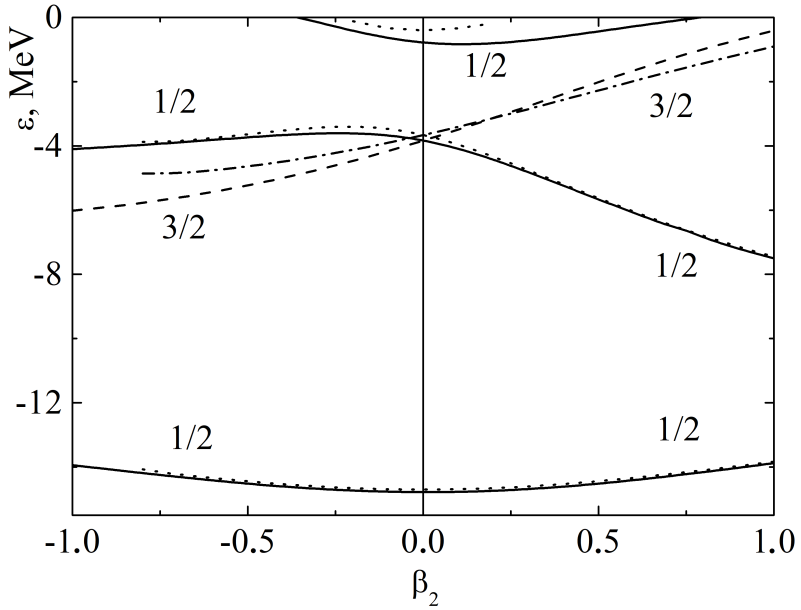

Figure 5. The dependence of energies of levels (values of $|m_j|$ are indicated) on the deformation parameter β_2 for the ^{8}Li nucleus: solid and dashed lines are calculations using expansion into series of Bessel functions; dotted and dash-dotted lines are calculations using the NRV Web Knowledge Base [4]. Values of parameters are the same as in Figure 4.

Calculations using expansion into series of Bessel functions and NRV Web Knowledge Base [4] were performed with the same values of parameters (Figure 5). The NRV Web Knowledge Base [4] may be useful for obtaining approximate results quickly, but without error evaluation (Figure 4).

For the positive value of the deformation parameter $\beta_2 = 0.5$, good agreement of the theoretical neutron separation energy with the experimental value (2.033 MeV [4]) was achieved. Significant decrease of separation energy compared with 7.25 MeV for ^{7}Li ($\beta_2 = -1.0$) may be explained by the opposite sign of the deformation $\beta_2 = +0.5$ for ^{8}Li (Figures 4, 5). The large difference between the separation energies may be explained by the different shapes of outer nucleon clouds. The probability densities for neutrons of the ^{8}Li nucleus for prolate and oblate shapes are shown in Figures 6 and 7, respectively. It can be seen that the shape of neutron cloud with quantum number $|m_j| = 1/2$ (Figure 5b) corresponds to the prolate shape of the ^{8}Li nucleus ($\beta_2 = +0.5$). The shape of the neutron cloud with the quantum number $|m_j| = 3/2$ (Figures 6c and 7b) corresponds to the oblate shape. It explains the different order of these energy levels for positive and negative deformations. Similarly, in the ^{7}Li nucleus, the probability density distribution for $|m_j| = 3/2$ level corresponds to the oblate shape (Figure 2b).

The probability density calculated in cylindrical coordinates for an outer neutron of ^{8}Li is close to the spherical shape (Figures 6c, 7c) and has similar spatial extent. It confirms the possibility of application of the spherical shell model to description of the weakly bound external neutrons in the ^{8}Li nucleus.

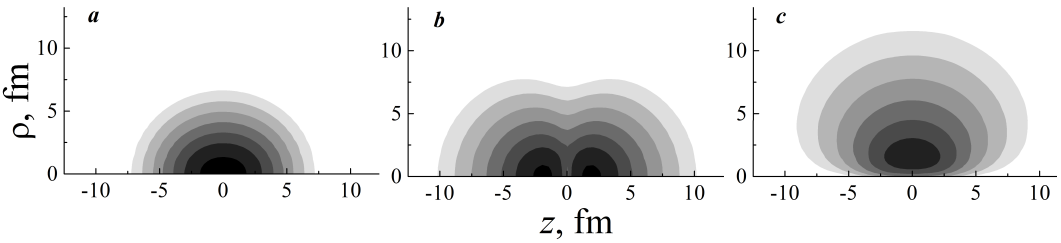

Figure 6. Probability density for the neutron levels with quantum numbers $|m_j| = 1/2$ (a), $|m_j| = 1/2$ (b), and $|m_j| = 3/2$ (c) in the deformed ^{8}Li nucleus in the model with prolate shape ($\beta_2 = +0.5, \beta_4 = 0$) obtained using expansion into series of Bessel functions. Panels a, b, c correspond to the increasing energy of levels, see Figure 5.

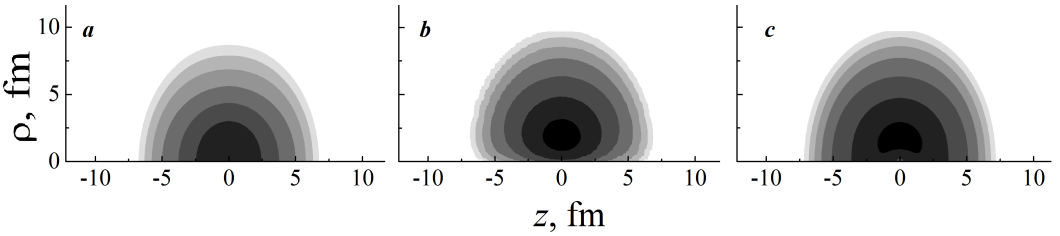

Figure 7. Probability density for the neutron levels with quantum numbers $|m_j| = 1/2$ (a), $|m_j| = 3/2$ (b), and $|m_j| = 1/2$ (c) in the deformed ^{8}Li nucleus in the model with prolate shape ($\beta_2 = -0.5, \beta_4 = 0$) obtained using the NRV Web Knowledge Base [4]. Panels a, b, c correspond to the increasing energy of levels, see Figure 5.

In the following section the spherical shell model calculations are described in detail.

The shell model of spherical nucleus

The effective central potential for neutron is written as

$$V_{\text{eff}}(r) = V(r) + \frac{\hbar^2 l(l+1)}{2mr^2}, \;\; l = 0, 1, ... \tag{11}$$

and for proton

$$V_{\text{eff}}(r) = V_{\text{C}}(r) + V(r) + \frac{\hbar^2 l(l+1)}{2mr^2}, \;\; l = 0, 1, ... \tag{12}$$

For the nuclear part of the potential $V(r)$, we used the Woods-Saxon form

$$V(r) = \frac{V_0^{(\text{WS})}}{1 + \exp\left(\frac{r - R^{(\text{WS})}}{a^{(\text{WS})}}\right)}, \tag{13}$$

where $R^{(\text{WS})} = r_0^{(\text{WS})} A^{1/3}$ is the radius of the potential well, $a^{(\text{WS})}$ is diffuseness of the potential well. The Coulomb potential $V_{\text{C}}(r)$ was represented in the model of uniformly charged sphere with radius R_{C}

$$V_{\text{C}}(r) = \begin{cases} \frac{(Z-1)e^2}{2R_{\text{C}}}\left[3 - \left(\frac{r}{R_{\text{C}}}\right)^2\right], \; r < R_{\text{C}}, \\ \frac{(Z-1)e^2}{r}, \; r \geq R_{\text{C}}, \end{cases} \tag{14}$$

where Z is the nucleus charge and e is elementary charge.

The total nucleon wave function taking into account spin-orbit interaction in the central field for all projections of the total angular momentum $|m_j|$ on the Oz axis [18] is a three-dimensional spinor

$$\Psi_{n,l,j,m_j}(r, \theta, \varphi) = \begin{pmatrix} \psi_1 \\ \psi_2 \end{pmatrix} \tag{15}$$

The explicit form of total nucleon wave function is

$$\Psi_{n,l,j_1,m_j}(r, \theta, \varphi) = \frac{1}{\sqrt{2l+1}} R_{n,l,j_1}(r) \begin{pmatrix} Y_{l,m_j-1/2}(\theta, \varphi)\sqrt{l + m_j + 1/2} \\ Y_{l,m_j+1/2}(\theta, \varphi)\sqrt{l - m_j + 1/2} \end{pmatrix}, \tag{16}$$

$$\Psi_{n,l,j_2,m_j}(r, \theta, \varphi) = \frac{1}{\sqrt{2l+1}} R_{n,l,j_2}(r) \begin{pmatrix} -Y_{l,m_j-1/2}(\theta, \varphi)\sqrt{l - m_j + 1/2} \\ Y_{l,m_j+1/2}(\theta, \varphi)\sqrt{l + m_j + 1/2} \end{pmatrix}, \tag{17}$$

where $R_{n,l,j}(r)$ are the radial functions. The total momentum j of the nucleon has values $j_1 = l + 1/2$ and $j_2 = l - 1/2$.

The probability density for a certain state with quantum numbers n, l, m_j is defined as

$$P_{n,l,j,m_j}(\vec{r}) = \left|\psi_1(r, \theta, \varphi)\right|^2 + \left|\psi_2(r, \theta, \varphi)\right|^2 \tag{18}$$

The radial Schrödinger equation has the form [10, 12]

$$y''(r) + \frac{2m}{\hbar^2}\left[\varepsilon - V_{\text{eff}}(r) - V_j(r)\right] y(r) = 0 \tag{19}$$

where $y(r) = rR_{n,l,j}(r)$. The spin-orbit potential $V_j(r)$ is

$$V_j(r) = \begin{cases} U^{(\mathrm{SO})}(r)(l+1)/2, j = j_2 = l - 1/2, \\ -U^{(\mathrm{SO})}(r)l/2, j = j_1 = l + 1/2, \end{cases} \tag{20}$$

where

$$U^{(\mathrm{SO})}(r) = b\frac{1}{r}\frac{dV^{(\mathrm{SO})}(r)}{dr}, \tag{21}$$

$$V^{(\mathrm{SO})}(r) = \frac{V_0^{(\mathrm{SO})}}{1 + \exp\left(\frac{r - R^{(\mathrm{SO})}}{a^{(\mathrm{SO})}}\right)}, \tag{22}$$

and $R^{(\mathrm{SO})} = r_0^{(\mathrm{SO})} A^{1/3}$.

In this work, all calculations of energies and radial wave functions in the shell model of spherical nucleus were carried out with using the program and algorithm presented in handbook [19]. Equation (19) was solved numerically with boundary conditions: $y(0) = 0$ and $y(r) \to 0$ at $r \to \infty$. The grid $r_k = 0.5h + kh, k = 0, ..., N$ (h is grid step, k is the number of grid point) and the grid function $y_k = y(r_k)$ were introduced. Derivatives in the differential equation (19) were approximated by linear combinations of function values at the grid points. For energy calculations, finite difference method was used

$$y''(r) \approx \frac{y_{k-1} - 2y_k + y_{k+1}}{h^2}. \tag{23}$$

Equation (23) leads to the eigenvalue problem for the tridiagonal matrix A:

$$\begin{aligned} &AY = \lambda Y, \\ &\lambda = \tfrac{2m}{\hbar^2}\varepsilon h^2, \\ &A_{kk} = 2 + h^2\left(\tfrac{2m}{\hbar^2}V_{eff}(r_k)\right), k = \overline{0,N}, A_{kk\pm1} = -1, \end{aligned} \tag{24}$$

where λ is an eigenvalue of the matrix, A_{kk} are diagonal matrix elements, $A_{kk\pm1}$ are subdiagonal matrix elements. The energies ε were calculated using the bisection method for matrix eigenvalues [19].

To evaluate the applicability and accuracy of the method, consider a system with an infinitely heavy core and a neutron with mass m. For this problem, the modified Pöschl-Teller potential is written

$$V_{\mathrm{PT}}(r) = -\frac{\hbar^2\alpha^2}{2m}\frac{\xi(\xi-1)}{\cosh^2(\alpha r)}, \tag{25}$$

where ξ, α are parameters. In this case, analytical expressions for the energy states of discrete spectrum are known [20]

$$E_n = -\frac{\hbar^2\alpha^2}{2m}(\xi - 2n)^2, \quad n = 1, 2, \ldots \tag{26}$$

In the units used in the nuclear scale

$$E_n = -\varepsilon_0 \frac{\hbar^2}{2m\varepsilon_0 x_0^2}\tilde{\alpha}^2(\xi - 2n)^2 = -b_0\tilde{\alpha}^2(\xi - 2n)^2 \qquad (27)$$

where $x_0 = 1$ fm, $\tilde{\alpha} = \alpha x_0$, $\varepsilon_0 = 1$ MeV, $b_0 = \varepsilon_0\hbar^2\left(2mx_0^2\right)^{-1} \approx 20.7296$ MeV. For $\tilde{\alpha} = 1$, $\xi = 3$, the exact result for $n = 1$ is $E_1 = -20.7296$ MeV. For $r_{\max} = 40.0$ fm and grid step $h = 10^{-5}$ fm, the bisection method yielded the value $E_1 = -20.7303$ MeV. The calculations using expansion into series of Bessel functions yielded the value –20.738 MeV.

For the parameters of the potential $V(r)$ (see Table 1 and Figure 8), the energies of the uppermost-occupied neutron and proton levels of the ^{8}Li nucleus were equal to the separation energies taken with the opposite sign. The experimental neutron and proton separation energies are 2.032 MeV and 12.416 MeV, respectively. Calculations were carried out with $r_0^{(WS)}$, $r_0^{(SO)}$, $a^{(WS)}$, $a^{(SO)}$, κ recommended parameters from [21]. The calculated single-particle energies ε for the ^{8}Li nucleus are shown in Table 2 and Figure 8.

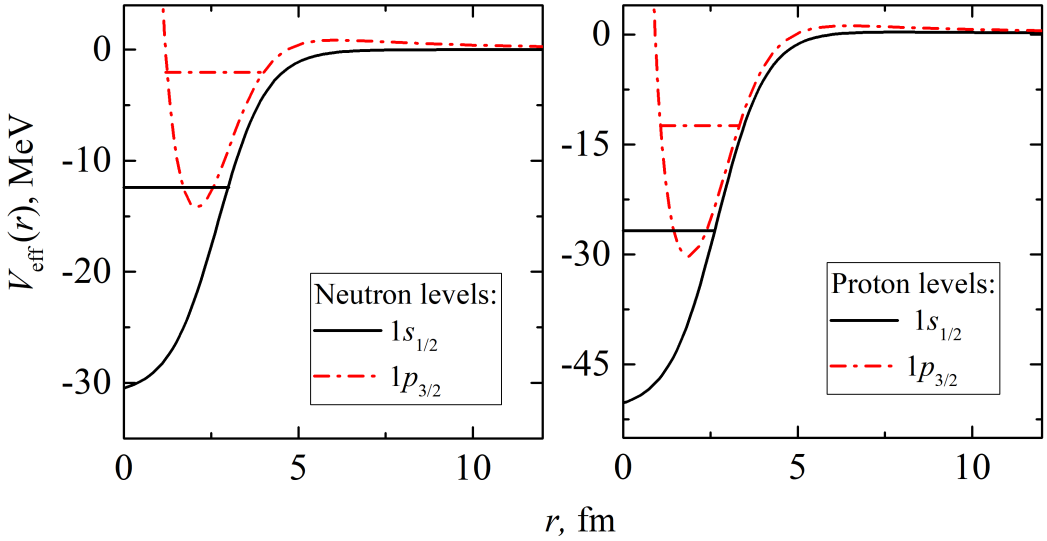

Figure 8. Effective potential and single-particle levels for neutron and proton of ^{8}Li nucleus.

Table 1.
Parameters of the potential for the ^{8}Li nucleus.

Neutrons		$V_0^{(WS)}$, MeV -31.115	$r_0^{(WS)}$, fm 1.347	$a^{(WS)}$, fm 0.7	
		$V_0^{(SO)}$, MeV -31.115	$r_0^{(SO)}$, fm 1.31	$a^{(SO)}$, fm 0.7	κ 35
Protons	R_C, fm 2.32	$V_0^{(WS)}$, MeV -52.964	$r_0^{(WS)}$, fm 1.347	$a^{(WS)}$, fm 0.7	
		$V_0^{(SO)}$, MeV -52.964	$r_0^{(SO)}$, fm 1.31	$a^{(SO)}$, fm 0.7	κ 36

Table 2.
The single-particle energies ε (MeV) for the ^{8}Li nucleus.

State	Neutrons	Protons
$1s_{1/2}$	–12.404	–26.764
$1p_{3/2}$	–2.032	–12.416

The radial functions $R_{n,l,j}(r)$ were calculated by integration from large values of radius to small values, see e.g. [22]. Results for neutron and proton wave functions are shown in Figure 9. The spatial extent of the external neutron wave function (see Figures 6c and 7c) and the low neutron separation energy (2.03 MeV) in the ^{8}Li nucleus can lead to the high probability of neutron transfer and breakup [11].

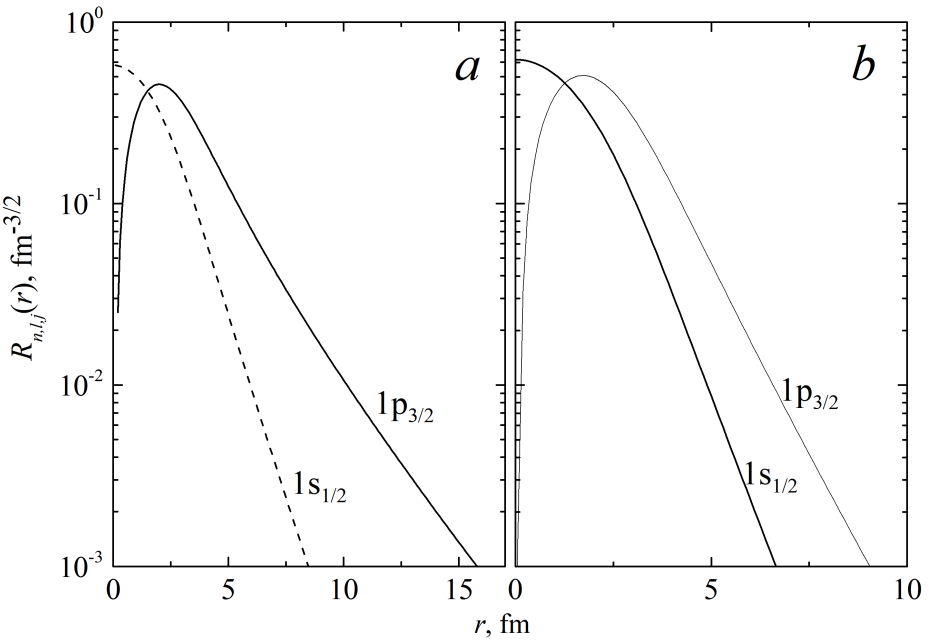

Figure 9. Radial functions $R_{n,l,j}(r)$ for neutron (a) and proton (b) levels $1s_{1/2}$ and $1p_{3/2}$ in the ^{8}Li nucleus (see Figure 8 and Table 2).

Conclusion

The energy levels of neutrons and protons and the corresponding probability densities for Li isotopes were calculated within the shell model of deformed and spherical nuclei. Using the calculated probability densities for neutrons, we have been able to explain the shape of ^{7}Li nucleus. The calculated probability densities for outer neutrons of ^{8,11}Li nuclei for deformed and spherical shapes exhibited similar spatial extent. These results demonstrate that the shell model of spherical nuclei may also be used for approximate description of the weakly bound external neutrons in ^{11}Li and ^{8}Li nuclei.

Acknowledgments

Acknowledgement This work was supported by the Ministry of Education and Science of the Republic of Kazakhstan within the program of funding research activities through grants for 2018–2020 «Experimental and theoretical research of the interaction of light weakly bound nuclei at low energies – for astrophysical applications» (grant no. 303 of March 29, 2018).

References

[1] Yu.E. Penionzhkevich, Physics of Atomic Nuclei **74** (2011) 1615.
[2] K.A. Kuterbekov, A.M. Kabyshev, A.K. Azhibekov, Chinese Journal of Physics **55** (2017) 2523.
[3] Yu.E. Penionzhkevich, Yu.G. Sobolev, V.V. Samarin, M.A. Naumenko, Physics of Atomic Nuclei **80** (2017) 928.
[4] V.I. Zagrebaev et al., NRV Web Knowledge Base on Low-Energy Nuclear Physics, http://nrv.jinr.ru/.
[5] A.V. Karpov et al., Physics of Atomic Nuclei **79** (2016) 749.
[6] A.V. Karpov et al., Nucl. Instrum. Methods Phys. Res. A **859** (2017) 112.
[7] V.G. Soloviev, Teoriya atomnogo yadra: yadernye modeli (Moscow: Energoizdat, 1981) 296 p. (in Russian)
[8] W. Von Oertzen, M. Freer, Y.K. En'yo, Phys. Rep. **432** (2006) 43.
[9] http://cdfe.sinp.msu.ru/services/radchart/radmain.html.
[10] A. Bohr, B.R. Mottelson, Nuclear Structure V. 2: Nuclear Deformations (Singapore, World Scientific, 1998) 749 p.
[11] Yu.E. Penionzhkevich, Yu.G. Sobolev, V.V. Samarin, M.A. Naumenko et al., Phys. Rev. C **99** (2019) 014609.
[12] Yu.M. Shirokov, N.P. Yudin, Yadernaya fizika (Moscow, Nauka, 1980) 728 p. (in Russian)
[13] Sir R. Peierls, Surprises in Theoretical Physics (Princeton, Princeton University Press, 1979) 176 p.
[14] M. Göppert -Mayer, J.Hans, D. Jensen, Elementary theory of nuclear shell structure (New York, John Wiley and sons, 1955) 291 p.
[15] V.I. Zagrebaev, V.V. Samarin, Physics of Atomic Nuclei **67** (2004) 1462.
[16] V.V. Samarin, Physics of Atomic Nuclei **78** (2015) 128.
[17] V.V. Samarin, M.A. Naumenko, Bull. Russ. Acad. Sci. Phys. **83**(4) (2019) 411.
[18] L.D. Landau, E.M. Lifshits, Kvantovaya mekhanika: Nerelyativistskaya teoriya V. 4 (Moscow, Nauka, 1973) 767 s. (in Russian)
[19] J.H. Wilkinson, C. Reinsch, Handbook for Automatic Computation Linear Algebra (Sprunger-Verlag, Berlin, 1971) 439 p.
[20] S. Flugge, Practical Quantum Mechanics I (Springer-Verlag, Berlin, 1971) 344 p.
[21] S. Cwiok et al., Computer Physics Communications **46** (1987) 379.
[22] V.V. Samarin, Bull. Russ. Acad. Sci. Phys. **78** (2014) 1124.